J Mater Sci (2007) 42:4406–4417
DOI 10.1007/s10853-006-0652-0

Novel sodium alginate composite membranes prepared by incorporating cobalt(III) complex particles used in pervaporation separation of water–acetic acid mixtures at different temperatures

Ravindra S. Veerapur · K. B. Gudasi · M. Sairam · R. V. Shenoy · M. Netaji · K. V. S. N. Raju · B. Sreedhar · Tejraj M. Aminabhavi

Received: 11 October 2005 / Accepted: 7 July 2006 / Published online: 28 February 2007

Abstract The present paper is our continuing effort to develop a new type of sodium alginate (NaAlg) composite membrane by incorporating cobalt(III)(3-acetylpyridine-*o*-aminobenzoylhydrazone) (Co-APABZ) complex as filler particles in different ratios. Membranes were prepared by solution casting followed by solvent evaporation and crosslinked with glutaraldehyde. Pervaporation (PV) performance of the prepared composite membranes was assessed in terms of flux and selectivity and these data were compared with the pristine NaAlg membrane in PV dehydration of water–acetic acid mixtures. Pristine Co-APABZ particles in crystalline form were prepared and characterized by the solid state X-ray diffraction (XRD) technique, while the NaAlg/Co(III)composite membranes were characterized by thermogravimetry (TGA) and dynamic mechanical thermal analyzer (DMTA). X-ray crystal structure of Co-APABZ has shown that the complex formed was crystalline in nature with six lattice water molecules, which are interconnected by hydrogen bonds linking together to form cyclic hexamers that are analogous to cyclohexane, creating water channels for an easy transport of water molecules. TGA indicated no changes in thermal stability of the membranes due to the presence of Co-APABZ in the NaAlg matrix. DMTA confirmed NaAlg crosslinking with glutaraldehyde. Effects of Co-APABZ content, membrane thickness, temperature and feed water compositions on membrane performance were investigated to find an optimum PV performance of the membranes developed. NaAlg composite membranes in the presence of Co-APABZ particles preferentially absorbed water molecules to facilitate diffusion of water through the membranes and thus enhance the selectivity to water. However, the amount of Co-APABZ present in the NaAlg matrix and the degree of membrane swelling has an effect on membrane performance. Selectivity of 174 for water with a flux of 0.123 kg/m^2 h was obtained for 5 wt.% Co-APABZ containing NaAlg matrix, when tested for the feed mixture containing 10 wt % water. The present results are superior to the previously published data based on NaAlg membranes.

This article is CEPS communication #110.

R. S. Veerapur · M. Sairam · T. M. Aminabhavi (✉)
Membrane Separations Division, Center of Excellence in Polymer Science, Karnatak University, Dharwad 580 003, India
e-mail: aminabhavi@yahoo.com

K. B. Gudasi · R. V. Shenoy
Department of Chemistry, Karnatak University, Dharwad 580 003, India

K. B. Gudasi
e-mail: kbgudasi@rediffmail.com

M. Netaji
Department of Inorganic and Physical Chemistry, Indian Institute of Science, Bangalore 560 012, India

K. V. S. N. Raju
Organic Coatings and Polymers Division, Indian Institute of Chemical Technology, Hyderabad 500 007, India

B. Sreedhar
Inorganic and Physical Chemistry Division, Indian Institute of Chemical Technology, Hyderabad 500 007, India

Introduction

Acetic acid is one of the most important intermediates used in chemical industries. As the relative volatility

of water to acetic acid is close to unity, much energy is required if one attempts to separate acetic acid from water by column distillation. On the other hand, pervaporation (PV) has been widely used as a technique to separate aqueous acetic acid mixtures [1, 2]. Separation of acetic acid–water mixtures by PV was reviewed by Aminabhavi and Toti [3]. Sodium alginate (NaAlg) and modified NaAlg membranes have been widely used in PV dehydration studies of organic–water mixtures [4–7]. In the earlier literature, Uragami and Saito [8] used the alginic acid membranes for PV separation of alcohol–water mixtures. Mochizuki et al. [9] studied the relationship between permselectivity of alginic acid membrane and its solid-state structure as well as the effect of counter cations on membrane performance. In another study, Yeom and Lee [10] used glutaraldehyde crosslinked NaAlg membrane for the PV separation of ethanol–water mixtures. Huang et al. [11] prepared the crosslinked NaAlg membranes using various divalent and trivalent metals for the PV separation of ethanol–water and isopropanol–water mixtures. Recently, Toti et al. [12, 13] prepared the blend membranes of NaAlg with polyacrylamide-*g*-guar gum for the PV separation of acetic acid–water and isopropanol–water mixtures. Several asymmetric membranes and thin film composites of NaAlg with different hydrophilic and hydrophobic support materials have been employed in PV applications [14–18]. In an effort to increase the PV performance of NaAlg, its blends with hydrophilic polymers like poly(vinyl alcohol), cellulose, etc., have been attempted [19].

It has been reported in the earlier literature [20–23] that addition of hydrophilic zeolites would improve the PV performance characteristics of the membranes. In continuation of our ongoing program of research to develop filled matrix membranes, we thought of synthesizing cobalt(III) complex particles prepared by reaction of $CoCl_2$ with 2-acetylpyridine-*o*-aminobenzoylhydrazone (Co-APABZ), which will exhibit propensity to create water channels as evidenced by X-ray data of the complex. Realizing that such water channels present in Co(III) complex molecule will further improve the membrane performance characteristics of NaAlg even if these are present in small quantities for dehydrating acetic acid. In this direction, we have undertaken the present research to develop novel type of composite membranes by incorporating Co-APABZ crystals in different amounts (2, 3 and 5 wt.%) with respect to weight of NaAlg. The developed membranes have enhanced the PV performances over that of the pristine NaAlg membrane while dehydrating acetic acid. Sorption experiments on the composite membranes have been performed to support the membrane performance results. The effect of varying amount of Co(III) complex particle loading, membrane thickness, temperature, and feed compositions have been investigated in detail in order to find the appropriate application of the developed composite membranes of NaAlg for the selective separation of water from acetic acid by the PV method.

Experimental

Materials

Sodium alginate, methanol, acetone, glutaraldehyde, HCl and $CoCl_2$ were all purchased from s.d. fine chemicals, Mumbai, India. Deionized water having a conductivity of 20 μS/cm was produced in the laboratory itself using the Permionics pilot plant (Vadodara, India) on a nanofiltration membrane module.

Preparation of (3-acetylpyridine-*o*-aminobenzoyl hydrazone)

o-Aminobenzaldehyde (1.51×10^{-2} kg, 0.1 M) was dissolved in 1.3×10^{-4} m^3 of methanol. 2-Acetyl pyridine (1.21×10^{-2} kg, 0.1 M) was then added to the above solution, which upon stirring for 3–4 h yielded a crystalline product. The product was isolated by filtration, washed with alcohol and dried in air. Recrystallization from hot methanol yielded yellow colored crystals of 3-acetylpyridine-*o*-aminobenzoyl hydrazone [APABZ].

Preparation of (3-acetylpyridine-*o*-aminobenzoyl hydrazone) Co(III) complex $[Co(APABZ)_2]Cl{\cdot}6H_2O$

Co(III) complex was prepared by adding 0.001 M $CoCl_2$ to a warm solution of 2-acetylpyridine-*o*-aminobenzoylhydrazone (APABZ) with continuous stirring. A thick precipitate was formed immediately, but stirring was continued for 5–6 h. The complex obtained was filtered, washed with aqueous alcohol and dried in air. The Co(II) has undergone oxidation to Co(III) upon complexation. Blackish red crystals suitable for X-ray diffraction studies were obtained by the slow evaporation of its methanolic solution.

Preparation of cobalt(III) complex-incorporated NaAlg membranes

Cobalt(III) complex-loaded NaAlg membranes were prepared by dissolving 4 g of NaAlg in 1×10^{-4} m^3 of

water for 24 h with constant stirring. To this solution, a required amount of Co(III) complex was added to 1×10^{-5} m^3 of water taken in a beaker and sonicated for 2 h. Cobalt(III) complex (2, 3 and 5 wt.% with respect to weight of NaAlg) was added to NaAlg solution and stirred for overnight. The mixture was cast as membranes on a clean glass plate, dried at room temperature and peeled off from the glass plate. The membranes were designated, respectively, as NaAlg/Co(III)-2, NaAlg/Co(III)-3 and NaAlg/Co(III)-5. Membranes formed were immersed in a bath containing water:acetone (30:70, v/v), 2.5×10^{-6} m^3 of glutaraldehyde, 2.5×10^{-6} m^3 of HCl and were allowed to crosslink for about 12 h. Membranes were removed from the crosslinking bath, washed with distilled water, and dried at room temperature. Membrane thicknesses were measured by micrometer screw gauge at different positions with standard errors being <±1.0 μm.

X-ray diffraction studies

The crystal structure of 3-acetylpyridine-*o*-aminobenzoyl hydrazone was determined with dimensions of $0.53 < \theta < 25.90°$. The CCDC deposit number is 269976. The crystal structure of Co(III) complex was determined by developing a crystal with dimension $0.71 \times 0.51 \times 0.26$ mm^3. Data were collected at 293 K with scan mode in the range $1.72 < \theta < 27.91$. A total of 18350 (7821 independent, R_1; 0.0604 and $\omega R_2 = 0.1269$) reflections were measured. The CCDC deposit number is 271781. The crystallographic data for 3-acetylpyridine-*o*-aminobenzoyl hydrazone and its complex with Co(III) are given in Table 1.

Thermogravimetric analysis (TGA)

TGA thermograms of the membranes were recorded on a Simultaneous Thermal Analysis (model 1500, Surrey, U.K) system. TGA scans were done from 298 to 1073 K at the heating rate of 293 K/min in an inert nitrogen atmosphere.

Dynamic mechanical thermal analysis (DMTA)

DMTA analyses of the pristine NaAlg, uncrossinked NaAlg/Co(III) and crossinked NaAlg/Co(III) membranes have been performed on a DMTA IV (Rheometric Scientific, USA) instrument operating at 1 Hz frequency between 298 K and 473 K at the heating rate of 278 K/min.

Table 1 Crystal data, data collection and structure refinement

	APABZ	$[Co(APABZ)_2]Cl{\cdot}6H_2O$
Empirical formula	$C_{14}H_{14}N_4O$	$C_{28}H_{38}N_8O_8CoCl$
Formula weight	254.29	709.04
Crystal size, mm	$0.53 \times 0.46 \times 0.18$	$0.71 \times 0.57 \times 0.26$
Crystal system	Orthorhombic	Triclinic
Space group	*Pbca*	*P*1
A, nm	1.1484(17)	1.1783(10)
B, nm	1.47591(2)	1.1839(10)
C, nm	1.51882(2)	1.2734(10)
A	90.0	90.689(13)
B	90.0	110.453(12)
Γ	90.0	106.79(13)
V, nm^3	257.46(6)	158.1(2)
Z	8.0	2.0
ρ calcd, (kg/m^3)	1312.1	1490
Absorption coefficient (mm^{-1})	0.087	0.690
F (000)	1072	740
Range (°) for data collection	2.62–25.90	–
Number of reflections measured	18863	18350
Number of unique reflections	2528	7281
R (int)	0.0592	0.0408
Number of observed reflections	1,591	5,495
Final *R* indices [$1 > 2\sigma(1)$]	0.0632	0.0604
Goodness-of-fit	0.801	1.069

Degree of swelling

The % degree of swelling was performed gravimetrically on all the membranes in 10, 20 and 30 wt.% of water-containing feed mixtures at 303 K. Initial mass of the circularly cut (dia = 25 mm) NaAlg and NaAlg/Co(III) composite membranes was measured on a single-pan digital microbalance (model AE 240, Mettler, Switzerland) sensitive to 1×10^{-8} kg. Samples were placed inside the specially designed airtight test bottles containing 2×10^{-5} m^3 of the test solvent. Test bottles were transferred to an oven maintained at the constant desired temperature. Dry membranes were equilibrated by soaking in different compositions of the feed mixture in a sealed vessel at 303 K for 48 h. Swollen membranes were weighed immediately after carefully blotting and weighing on a digital microbalance. The % degree of swelling, DS was calculated as,

$$\%\mathrm{DS} = \left(\frac{W_\infty - W_0}{W_0}\right) \times 100 \quad (1)$$

where W_∞ and W_0 are the weights of swollen and dry membranes, respectively.

Sorption selectivity ($\alpha_{sorption}$)

To compute sorption selectivity, completely equilibrated membranes with different wt.% of water in the binary mixtures were removed from the test bottles and after blotting off the surface adhered liquid drops with a filter paper, they were placed in a glass trap surrounded by liquid nitrogen and then heated close to the boiling temperature of the organic liquid under consideration. The vapor was condensed in a cold trap surrounded by liquid nitrogen jar. Composition of the condensed liquid mixtures was then calculated by Nucon gas chromatograph (model 5765, Mumbai, India) provided with a thermal conductivity detector (TCD) equipped with a DEGS or Tenax packed column of 3.18 mm ID having 2 m length. Sorption selectivity was then calculated using:

$$\alpha_{sorp} = \frac{M_w/M_{organic}}{F_w/F_{organic}} \quad (2)$$

where M_w, $M_{organic}$ and F_w, $F_{organic}$ are wt.% of water and organic liquid (acetic acid) in the membrane and feed, respectively.

Pervaporation experiments

Pervaporation experiments have been performed on a 1×10^{-4} m^3 batch level manifold using an indigenously constructed instrument that was operated at a vacuum level up to 6.67 Pa in the permeate line (see Fig. 1). The effective membrane surface area was 1.993×10^{-3} m^2 and weight of the feed mixture taken in PV cell was 0.07 kg. Temperature of the feed mixture was maintained constant by a thermostatic water jacket. Before starting the PV experiment, test membrane was equilibrated for at least 2–4 h with feed mixture media. After establishment of steady state, permeate vapors were collected in cold traps immersed in liquid nitrogen up to 4–5 h. Weight of the permeate collected was measured on a Mettler Balance (model B 204-S, Greifensee, Switzerland: accuracy 10^{-7} kg) to determine the flux, J (kg m^{-2} h^{-1}) using weight of liquids permeated, W (kg), effective membrane area, A (m^2) and measurement time, t (h) as:

$$J = \frac{W}{At} \quad (3)$$

Analysis of feed and permeate samples was done using Nucon gas chromatograph (model 5765) provided with a TCD and equipped with a DEGS or Tenax packed column of 3.18 mm ID having 2 m length. Oven temperature was maintained at 343 K (isothermal), while injector and detector temperatures were maintained at 423 K. The sample injection volume was 1×10^{-9} m^3. Pure hydrogen was used as a carrier gas at a pressure of 10.66 psi. GC response was calibrated for column and for known compositions of water + acetic acid mixtures. Calibration factors were fed into the GC software to obtain the analysis for unknown samples. The pervaporation selectivity, α_{PV} was then calculated using,

$$\alpha_{PV} = \left(\frac{P_A}{1-P_A}\right)\left(\frac{F_A}{1-F_A}\right) \quad (4)$$

where F_A is mass % of water in feed and P_A is mass % of water in permeate. A minimum of three independent measurements of flux and α_{PV} were taken under similar conditions of temperature and feed compositions to confirm the steady-state pervaporation.

Results and discussion

X-ray diffraction studies

ORTEP and molecular packing diagrams of cobalt(III) complexes are depicted in Figs. 2–4. The molecule is coplanar, wherein Co(III) ion is bonded through O(1), N(1), O(1a) and N (1a), which occupy the equatorial sites, but N(2a) and N(2) occupy axial sites, indicating a distorted octahedral geometry around the metal center (Fig. 2). Co(III) complex tend to crystallize with six lattice water molecules. The crystal structure of Co(III) complex indicates its coplanarity. The Co(III) ion is bonded through O(1), N(1), and O(1a), which occupy the equatorial sites, while N(2a) and N(2) occupy the axial sites, indicating a distorted octahedral geometry around the metal center. The equatorial Co(I)–N(1) and Co(1)–N(1a) distances are 0.1920 nm and 0.1925 nm, which are significantly longer than the axial Co(1)–N(2a) and Co(1)–(2a) distances i.e., 0.1816 nm and 0.1816 nm. The Co(I)–O (1a) and Co(1)–O(1) bond distances are 0.1935 nm and 0.1909 nm, respectively. These values are typical of low-spin octahedral cobalt complexes [24, 25]. The distortion from ideal octahedral geometry is evidenced by the ''bite'' angles [N(1a)–Co(1)–N(2a): 82.48, O(1a)Co(1)–N(2a): 81.64, O(1)–Co(1)–N(1a): 90.15,

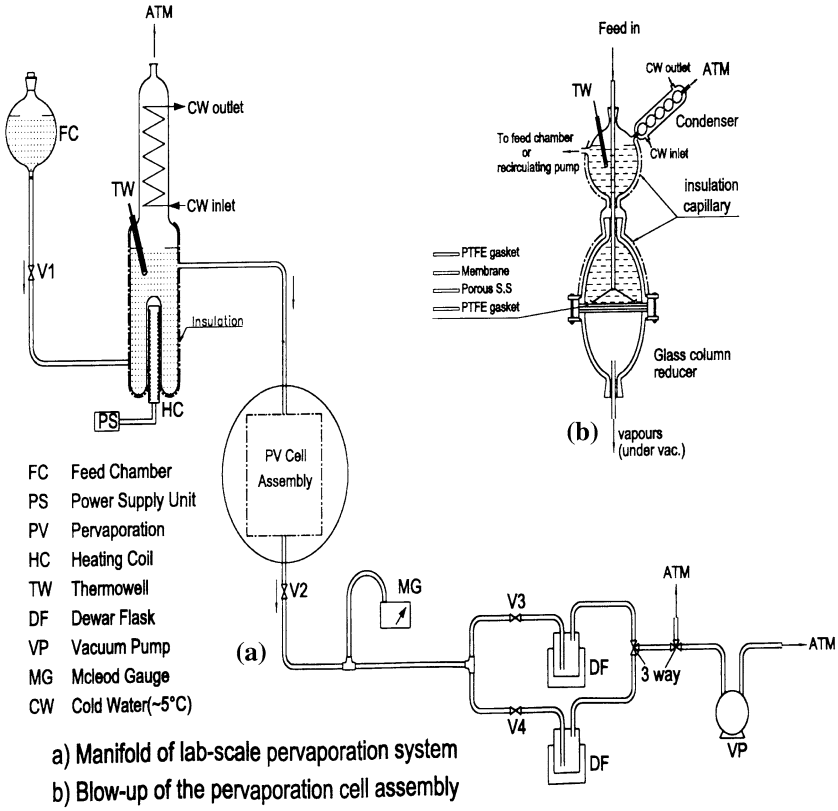

Fig. 1 Schematics of pervaporation unit

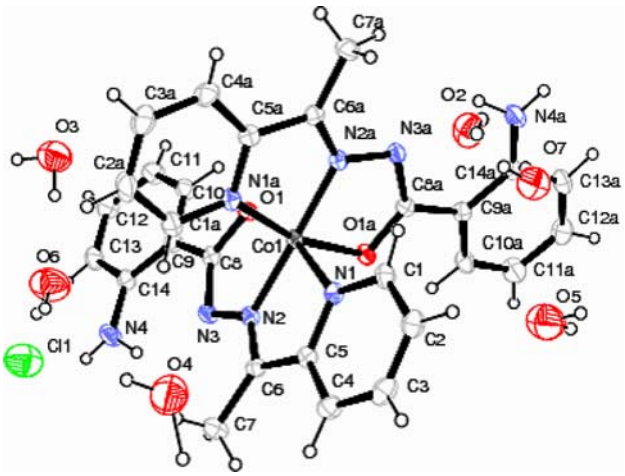

Fig. 2 ORTEP of $Co(APABZ)_2Cl{\cdot}6H_2O$

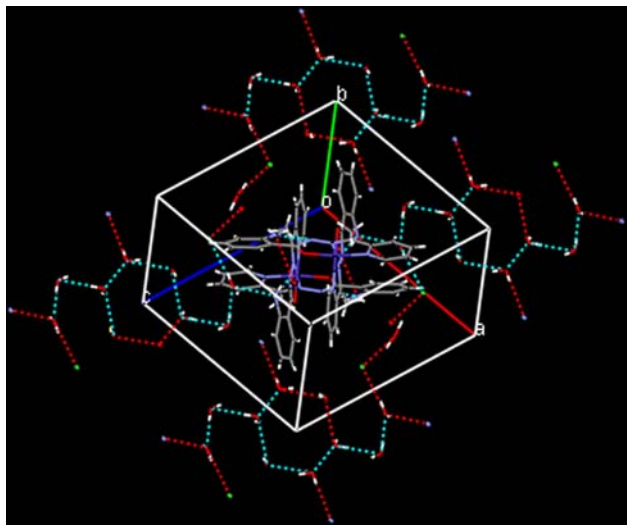

Fig. 3 Molecular packing diagram of $Co(APABZ)_2Cl{\cdot}6H_2O$ showing water hexamers

O(1)–Co(1)–N(2a): 81.68 and N91)–(Co1)–O(1a): [89.89°]. However, Co(III) atom does not deviate much from the best least squares plane defined by N(1), N(2), O(1), N(1a), N(2a) and O(1a). The coordinating atoms N(1), N(1a), O(1a) and O(1) form the equatorial plane, whereas N(2)–Co(1)–O(1a) [89.89°], N(1)–Co(1)–N(1a) [92.39°], N(1a)–Co(1)–O(1) [90.15°] and O(1)–Co(1)–O(1a) [91.96°]. The axial bond angle [N(2)–Co(1)–N(2a)—178.05°] is almost close to linear (180°). The N(2)–Co(1)–N(2a) bond angle is 178.05°, which is almost close to linearity (180°). On the other hand, axial coordinating atoms along with the central Co(III) atom deviate from linearity with angles of 164.09 [N(1)–Co(1)–O(1)] and 164.12° [O(1)–Co(1)–N(1a)].

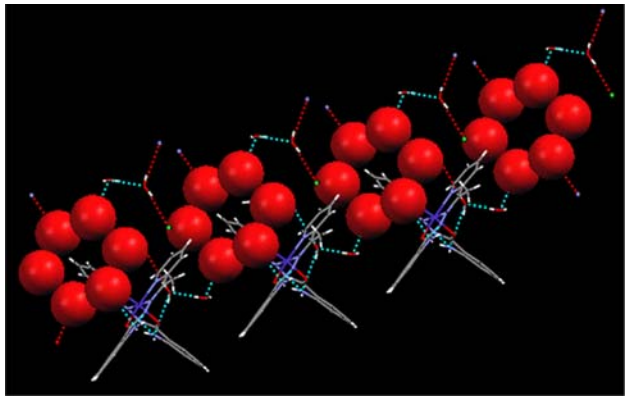

Fig. 4 A stereo regular view of the channel formed by water hexamers shown in space filling mode

The plane I comprising of C(9), C(10), C(11), C(12), C(13) and C(14) makes dihedral angles of 89.59°, 11.88° and 87.27° with plane II [C(9a), C(10a), C(11a), C(12a), C(13a), C(14a)], plane III [N(1), C(1), C(2), C(3), C(4), C(5) and C(6), N(2), Co(1)] and plane IV [N(1a), C(1a), C(2a), C(3a), C(4a), C(5a) and C(6a), N(2a), Co(1)], respectively. The following conformational changes are observed in the Co(III) complex. The C=O [O(1)–C(8) and O(1a–C8a)] are increased to 0.1308 nm compared to 0.1227 nm in free legand due to enolization and deprotonation effects. This is indicated by the changes in conformations across N(3)–C(8)–C(9)–C(14) and N(3)–N(2)–C(6)–C(7), which are +synperiplanar and –synperiplanar; torsional angles are +12.29 and –1.49°, respectively. These changes bring N(3), C(7) and C(4) [which were earlier in a *trans* positions to each other in legand] to *cis* positions upon complexation. Due to rotation about C(8)–N(3) bond, the N(4) of NH_2 group is *trans* to O(1). A decrease on ''bite'' distances of 0.2466 nm [O(1)–N(2)], 0.2496 nm [N(1)–N(2)], 0.2472 nm [O(1a)–N(2a)] and 0.2505 nm [N(1a)–N(2a)] is observed as compared to free ligand.

As expected from the potential donor atoms derived from two ligands, a chloride ion and six lattice held water molecules, a number of hydrogen bonds are observed in the molecule. One of the hydrogens of N(4) [NH_2 group] is involved in bifurcate hydrogen-bonding with O(1) (intermolecular) and N(3) (intramolecular), whereas other hydrogen is bonded to O(3) of water molecule. A similar hydrogen-bonding interaction is also observed in the second ligand molecule where one of the hydrogens of N(4) is hydrogen bonded to O(5) of the lattice water molecule. Similarly, the hydrogen of N(4) [NH_2 group] is also involved in bifurcate hydrogen-bonding with O(1A) (intermolecular) and O(3) (intramolecular), whereas other hydrogens of N(4) is hydrogen-bonded to O(5) of the lattice water molecule. Water clusters that known to cause structural changes of water molecule in their isolated and bulk states, via hydrogen-bonding may lead to various geometries that will line up to form water channels [26]. Further, systems containing such water channels might mimic ion and water membrane channels, analogous to aquaporin water channels [27]. These aquaporins are a series of homologous water channels composed of proteins and expressed in many epithelial, endothelial and other tissues. In general, water clusters are present in various isomeric forms, of which water hexamer is particularly interesting. These hexamers exist in various forms like cages, prisms, book boat and cyclic forms [28]. The water hexamer clusters are isoenergetic, i.e., all the forms have energies within 2.94 kJ/mol of each other. The lowest energy conformer is the cage followed by the book, prism, ring and bag, albeit at high temperatures, the population of the five hexamers is almost the same.

The present Co(III) complex crystallizes with six lattice water molecules. An interesting observation is that these water molecules are interconnected by a series of hydrogen-bonds, which link together to form cyclic hexameric forms analogous to cyclohexane molecule, each of O(2), O(5) and O(7) (Figs. 3 and 4) reveals such hexameric water molecules to form the extended water channels in the crystal structure between two layers of the complex molecule. These water channels have an appropriate width of 0.5 nm to 0.7 nm. Each hexamer is connected to the host molecule through two O(7) and O(5) water molecules with O(2) molecules remaining free. The O(7) is hydrogen-bonded to N(4a) of the host molecule in the adjacent layer, whereas O(5) is hydrogen-bonded to O(3), which in turn is bonded to O(6) water molecule. The O(6) is further involved in hydrogen-bonding with N(4) of an adjacent molecule as well as chloride ion. The chloride ion is further bonded to O(4) water molecule. Thus, O(3), O(4) and O(6) water molecules do not form a hexamer, but serve to support the cyclic hexamer formed by O(2), O(5) and O(7) by connecting it to the host. The hydrogen-bond angles of the water the molecules are close to linear, O–H–O, ranging from 168–176° and the O···O distances range 0.2710 nm to 0.2850 nm, compared to the corresponding value in ice, which is 0.2759 nm at –363 K. Similarly, O–O–O angles vary considerably from 87°–117°, which is appreciably distorted from the values in hexagonal ice, wherein these values are 109.3° [27]. Further, O(3)···O(6), O(5)····O(7), O(7)···O(2), O(2)···O(5) bond distances of 0.2713 nm, 0.2796 nm, 0.2852 nm and 0.2953 nm suggest the presence of strong intramolecular hydrogen-bonding between these oxygen atoms.

Thermogravimetric analysis (TGA)

TGA thermograms of cobalt(III) complex, pristine NaAlg and uncrosslinked NaAlg/Co(III) composite membranes are shown in Fig. 5. TGA thermogram of the pristine NaAlg membrane shows it to be stable up to 508 K. An initial weight loss of about 6 % was observed due to the release of moisture from the polymer. A weight loss of about 46% was observed between 503 K and 537 K due to degradation of the polymer (Fig. 5b). Thermogram of cobalt(III) complex shows a three-step degradation with an initial weight loss of 12.3% observed between 348 K and 385 K due to the release of bound water molecules because Co(III) complex contains water molecules; these water molecules are interconnected through a series of hydrogen-bonds (channels), which link together to form the cyclic hexameric forms. TGA thermograms show that major weight loss of 31% observed between 508 K and 588 K is due to the degradation of chelating agent (Fig. 5a). On the other hand, thermogram of NaAlg/Co(III)-5 membrane shows an initial weight loss of about 7.5% between 298 K and 384 K due to the release of moisture from the polymer as well as due to the release of water bound to Co(III) complex present in the NaAlg matrix. Notice that the onset of degradation of NaAlg is not affected by incorporating Co(III) complex into NaAlg matrix, but weight loss decreased from 46 to 33% (see Fig. 5c).

Dynamic mechanical thermal analysis (DMTA)

The tan δ curve of the pristine NaAlg membrane shows a glass transition temperature (T_g) of 382 K (see Fig. 6). However, the T_g of NaAlg did not change upon loading Co(III) complex particles into NaAlg, but T_g has shifted to 393 K after crosslinking with glutaraldehyde (see Fig. 7). The room temperature modulus of NaAlg membrane (460×10^3 MPa) has increased by one order of magnitude due to crosslinking of NaAlg membrane with glutaraldehyde.

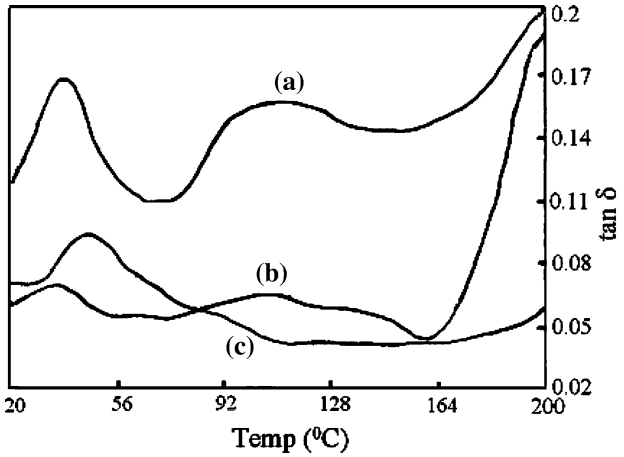

Fig. 6 Tan δ curves of (**a**) plain NaAlg, (**b**) uncrosslinked NaAlg/Co(III)-5 and (**c**) crosslinked NaAlg/Co(III)-5 membranes

Degree of swelling

The % degree of swelling obtained from swelling experiments at 303 K for pristine NaAlg and composite NaAlg membranes measured as a function of wt.% of water in the feed mixture is displayed in Fig. 8. Swelling kinetics depends upon the mutual diffusion of solvent molecules in response to polymer chain

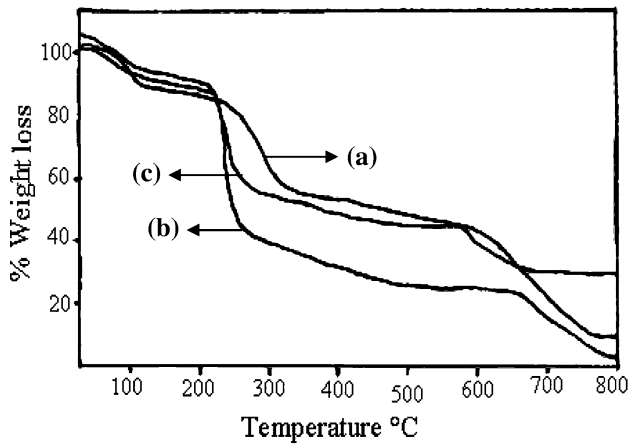

Fig. 5 TGA thermograms of (**a**) Co(III)complex, (**b**) plain NaAlg and (**c**) uncrosslinked NaAlg/Co(III)-5

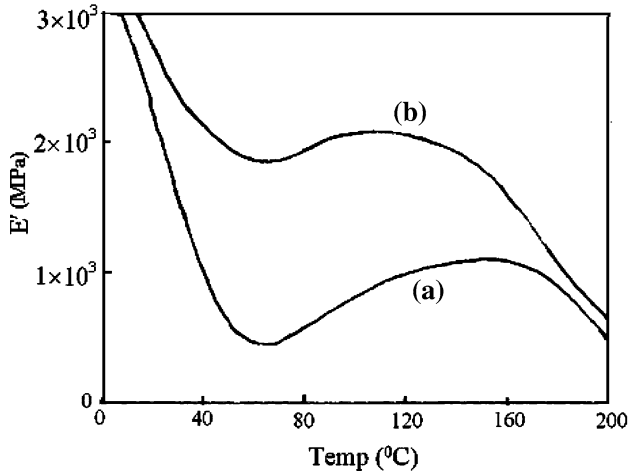

Fig. 7 E' curves of (**a**) pristine NaAlg, (**b**) crosslinked NaAlg/Co(III)-5 membranes

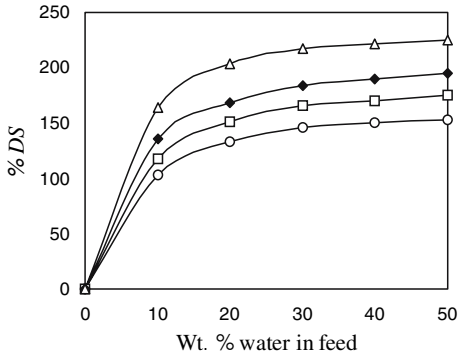

Fig. 8 Degree of swelling versus weight % of water in the feed. (○) pristine NaAlg, NaAlg/Co(III)-2 (□), NaAlg/Co(III)-3 (◆) and NaAlg/Co(III)-5 (△) membranes

relaxation processes [29]. In the present study, swelling increases with increasing loadings of Co(III) complex particles. For instance, swelling is higher for NaAlg/Co(III)-5 membrane than those observed for NaAlg/Co(III)-3 and NaAlg/Co(III)-2 membranes; for all the composite membranes, swelling is higher than the pristine NaAlg membrane. These data indicate that water molecules get sorbed preferentially and diffuse more easily through the composite membranes than pristine NaAlg membrane due to the availability of pores created by the addition of Co(III) complex particles. At higher water feed concentrations, amorphous regions of the membrane are highly swollen; hence, polymer chain becomes more flexible, thereby giving a decrease in diffusive transport of water molecules with increasing flux.

Effect of Co(III) complex content

It is well known that by introducing polar monomers like acrylamide into NaAlg backbone, it will lead to an improvement in PV performance of the overall membrane due to the effect of chemical grafting [12]. In order to improve the PV performance of NaAlg membrane to selectively separate water from acetic acid, we have developed the composite membranes loaded with different amounts of Co(III) complex. In order to test the stability of such membranes, we have soaked them in aqueous acetic acid to observe any possible leaching of the complex particles from the membranes. The UV-visible spectra of the aqueous acetic acid solution were recorded to detect any presence of Co(III) ion the in aqueous acetic acid solution. The absorption peak of Co(III) ion was not found in 90 wt.% aqueous acetic acid solution, suggesting that leaching of Co(III) ions did not take place and hence, NaAlg/Co(III) complex composite membranes are stable and intact during PV conditions.

The effect of Co(III) complex content of the membrane was tested to study the PV performance (see Fig. 9). It is observed that both flux and selectivity have increased with increasing amount of Co(III) complex particles in the membrane. Membranes were stable up to 5 wt.% of Co(III) complex loading into NaAlg and hence, the present study was limited to adding up to 5 wt.% of Co(III) complex particles in NaAlg matrix. The observed increase in selectivity is due to increased polymer chain packing density by adding increasing amount of Co(III) complex particles in NaAlg membrane. By comparing PV performances of NaAlg/Co(III) composite membranes with that of pristine NaAlg membrane, we find that NaAlg membrane containing 5 wt.% of Co(III) complex exhibited an improved PV performance over that of the pristine NaAlg membrane as well as other NaAlg composite membranes with lower loadings of Co(III) complex. Highest selectivity of 174 and flux of 0.123 kg/m^2 h were observed for NaAlg membrane containing 5 wt.% Co(III) complex. These results are in conformity with the sorption data discussed before.

Effect of feed composition

Flux and selectivity results are displayed in Table 2. The flux of pristine NaAlg membrane increased from 0.051 kg/m^2 h to 0.119 kg/m^2 h for feeds containing 10–30 wt.% of water in water–acetic acid feed mixtures. Upon increasing water content of the feed mixture from 10 to 30 wt.%, selectivity of pristine NaAlg membrane decreased from 18 to a much lower value of 3. Parallel to this effect, wt.% of water in permeate also decreased from a lower value of 67.18 to a still lower value of 55.76%. However, increase in flux with increasing amount of water in the feed is attributed to plasticization effect of the membrane due to swelling, thus allowing permeation of only water molecules from

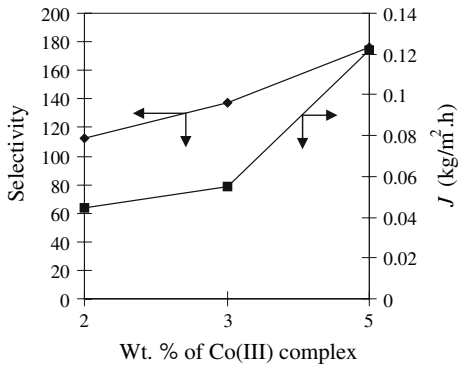

Fig. 9 Flux and selectivity versus % complex content (0, 2, 3, and 5 wt.%) for 10 wt.% of water in the feed

Table 2 Pervaporation results of water + acetic acid mixtures at 303 K under 6.67 Pa vacuum pressure

Wt.% of water in the feed	Flux J (kg/m^2 h)	Selectivity (α)	Wt.% of water in the permeate
Pristine NaAlg membrane			
10	0.051	18	67.18
20	0.094	7	62.83
30	0.119	3	55.76
NaAlg/Co(III)-2			
10	0.079	64	87.65
20	0.137	24	85.59
30	0.192	13	84.48
NaAlg/Co(III)-3			
10	0.096	79	89.82
20	0.173	28	87.63
30	0.262	15	86.27
NaAlg/Co(III)-5			
10	0.123	174	95.09
20	0.236	40	90.83
30	0.315	19	88.87

feed mixture through the membrane. However, PV performance of the pristine NaAlg membrane was improved by adding different amounts Co(III) complex particles (i.e., 2, 3 and 5 wt.%). For instance, the flux for NaAlg/Co(III)-2 membrane was increased from 0.079 to 0.192 kg/m^2 h, while for NaAlg/Co(III)-3, it increased from 0.096 to 0.262 kg/m^2 h with increasing amount of water in the feed from 10 to 30 wt.%. In case of NaAlg/Co(III)-5 membrane, flux was increased from 0.123 to 0.315 kg/m^2 h (see data presented in Table 2 and displayed in Fig 10). Water

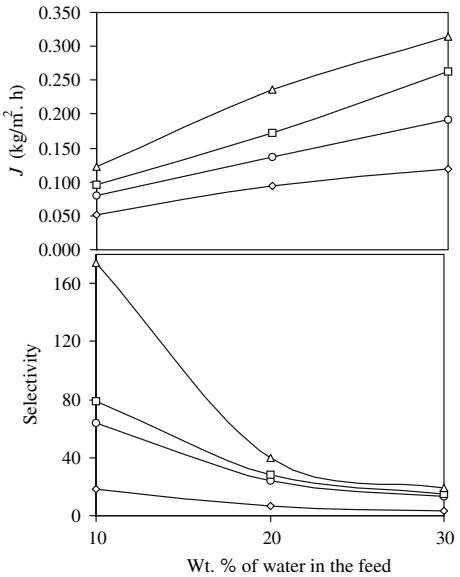

Fig. 10 Flux and selectivity versus weight % of water in the feed for water + acetic acid. Symbols: (○) pristine NaAlg, NaAlg/Co(III)-2 (□), NaAlg/Co(III)-3 (◆) and NaAlg/Co(III)-5 (△) membranes

removed on permeate side in case of NaAlg/Co(III)-2 membrane ranged between 87.65% and 84.48%, while for NaAlg/Co(III)-3 membrane, it ranged between 89.82% and 86.27%; on the other hand, for NaAlg/Co(III)-5, the amount of water extracted towards permeate side is higher, i.e., it ranged between 95.09% and 87.87% over the studied water compositions of the feed mixture. Such an increase in flux due to preferential absorption of water molecules as a result of water channels intrinsically created in Co(III) complex are further adding to the effect of increased water transport.

At 30 wt.% of water in feed, the selectivity is 19 for NaAlg/Co(III)-5 composite membrane, which is much higher than observed for pristine NaAlg membrane; however, a selectivity of only 3 is found for 30 wt.% water containing feed mixture. This suggests that the amount of Co(III) complex present in NaAlg matrix plays an important role in creating extra free channels within NaAlg matrix along with the additional water channels that are already created or aligned in Co(III) complex. This would allow for a better preferential absorption of water molecules within the interstices of Co(III) complex and Co(III) complex loaded NaAlg membranes, leading to increased flux and selectivity data. The decrease in selectivity with increasing amount of water in the feed is attributed to increased membrane swelling at higher concentrations of water in the feed. For instance, the selectivity of NaAlg/Co(III)-2 membrane decreased from 64 to 13 with increasing water concentration of the feed from 10 to 30 wt.%. Similarly, the selectivity values of NaAlg/Co(III)-3 and NaAlg/Co(III)-5 membranes decreased from 79 to 15 and 174 to 19, respectively under similar feed water concentrations. Selectivity and flux data exhibited by NaAlg/Co(III) composite membranes are higher than those of the pristine NaAlg membrane at all compositions of water in the feed. From these results, it is evident that both Co(III) complex content and membrane swelling contribute jointly in improving the PV performance of the composite membranes over that of the pristine NaAlg membrane.

Effect of membrane thickness

To study the effect of membrane thickness, we have typically selected the membrane (NaAlg/Co(III)-5), which gave high selectivity and high flux. Membranes of thicknesses of 25 μm, 50 μm, 80 μm, 120 μm, and 140 μm were prepared and subjected to PV experiments performed typically for 10 wt.% water in the feed mixture. It is observed that flux reduced systematically from 0.272 kg/m^2 h to 0.021 kg/m^2 h with

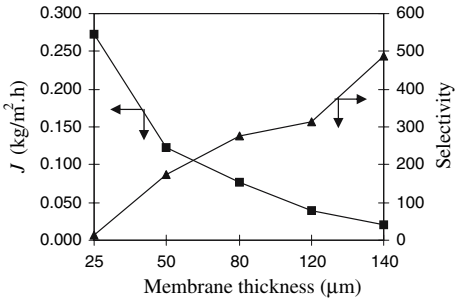

Fig. 11 Flux and Selectivity versus membrane thickness. (■) flux and (▲) selectivity

increasing membrane thickness from 25 μm to 140 μm. Figure 11 clearly displays this effect; for instance, a gradual decrease in flux with an increase in membrane thickness under identical operating conditions is observed. In PV, diffusion is the rate-controlling step, which decreases with increasing membrane thickness, thereby causing a subsequent reduction in flux. However, corresponding selectivity values increased from 13 to as high as 488 upon increasing membrane thickness from 25 to 40 μm. In PV process, the upstream layer of the membrane is swollen and plasticized due to absorption of feed liquid molecules, but allows only the unrestricted transport of feed components. In contrast, the downstream layer is virtually dry due to a continuous evacuation in permeate side and therefore, this layer forms the restrictive barrier, which allows only certain species (particularly, water in the present case) to transport across the membrane. It is expected that thickness of the dry layer will increase with increasing membrane thickness, thereby resulting in an improved selectivity as observed in the present study. Similar effects have also been observed in our earlier reports [30, 31].

Effect of temperature

To test the stability of all the membranes at higher temperatures viz., 313 K, 323 K and 333 K, PV experiments were performed for 10 wt.% of water containing feed mixtures. These data are reported in Table 3. It is observed that flux values increased with increasing temperature due to an increase of vapor pressure. However, the increased mobility of diffusing molecules as well as the polymer chain segmental mobility at higher temperatures is responsible for this type of effect. According to free volume theory [32], an increase in temperature increases the thermal mobility of the membrane polymer chains, which will create extra free volumes within the membrane matrix. This will further increase the sorption and diffusion rates of the permeating molecules, thus resulting in an easy transport of organic component from the feed mixture. On the other hand, membrane selectivity to water is reduced with increasing flux [33].

Permeation flux data obtained at different temperatures have been fitted to Arrhenius type relationship to estimate the activation parameters.

$$J_p = J_{p0} \exp(-E_p/RT) \tag{5}$$

Here, E_p is the activation energy for permeation, J_{p0} is permeation rate constant, R is molar gas constant and T is temperature in Kelvin. If activation energy values are positive, then flux will increase with increasing temperature. As the temperature increases, vapor pressure on the feed side of the membrane will also increase, whereas on the permeate side, vapor pressure will remain constant. This will result in increasing driving force at higher temperatures. Arrhenius plots of ln J_p vs. $1/T$ are linear as displayed in Fig. 12, suggesting that the temperature dependence of total permeation flux follows the Arrhenius rule, a trend that has also been observed in many earlier reports [34]. The calculated E_p value for pristine NaAlg membrane is 26.42 kJ/mol, whereas for NaAlg/Co(III)-5 membrane, a quite smaller value of E_p of 13.51 kJ/mol is observed. This indicates that composite membranes with a high selectivity have a smaller value of E_p than the pristine NaAlg membrane; this is due to lesser energy required for water molecules to cross over the Eyring's energy barrier. From the results of E_p given in Table 3, one can see that E_p values decrease systematically with increasing loadings of Co(III) complex particles. As expected, flux has increased with increasing temperature, but selectivity showed a reverse trend.

Diffusion selectivity

In the previous literature, sorption and diffusion model has been used to explain the PV transport of liquids through polymer membranes [35]. For the diffusive transport to take place, the presence of concentration gradient across the membrane is responsible. Therefore, one can calculate diffusion coefficient, D_i of the transporting liquid molecules through the membrane using the following Fick's equation [29].

$$J_i = p_i[p_{i(\text{feed})} - p_{i(\text{permeate})}] = \frac{D_i}{h}[C_{i(\text{feed})} - C_{i(\text{permeate})}] \tag{6}$$

Table 3 Pervaporation results of water + acetic acid mixtures at higher temperatures under 6.67 Pa vacuum pressure

Temperature (K)	Flux J (kg/m^2 h)	Selectivity (α)	Wt.% water in the permeate	E_p (kJ/mol)
Pristine NaAlg membrane				
303	0.051	18	67.18	26.42
313	0.076	15	62.81	
323	0.097	11	55.10	
333	0.112	8	47.55	
NaAlg/Co(III)-2				
303	0.079	64	0.079	21.45
313	0.103	42	0.103	
323	0.128	28	0.128	
333	0.149	21	0.149	
NaAlg/Co(III)-3				
303	0.096	79	0.096	17.74
313	0.118	50	0.118	
323	0.135	31	0.135	
333	0.165	23	0.165	
NaAlg/Co(III)-5				
303	0.123	174	0.123	13.51
313	0.138	92	0.138	
323	0.151	63	0.151	
333	0.187	47	0.187	

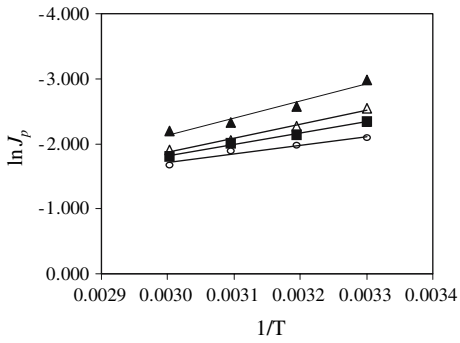

Fig. 12 Arrhenius plots of ln Jp vs 1/T at 10 wt.% of water in feed. (▲) pristine NaAlg, NaAlg/Co(III)-2 (△), NaAlg/Co(III)-3 (■) and NaAlg/Co(III)-5 (○) membranes

Here, C_i(feed) and C_i(permeate) are, respectively, the composition of liquids in feed and permeate sides. From the computed values of D_w and D_o (see Table 4), D_α($\equiv D_{water}/D_{organic}$) was calculated at 303 K. As expected, diffusion coefficients of water will increase considerably with an increasing amount of water in the feed mixture. Even though similar trends were observed for acetic acid, but diffusion coefficients of acetic acid are smaller when compared to diffusion values of water. The increase in diffusion coefficients of water and acetic acid with increasing water content of the feed mixture is attributed to the creation of extra free volume in the membrane matrix. It may be noticed that diffusion coefficients will increase with increasing amount of Co(III) complex particles in NaAlg, i.e., D_w values will increase systematically due to an increasing amount of Co(III) complex particles. The sorption and diffusion selectivity values are presented in Table 5. Diffusion selectivity decreased systematically with increasing amount of water in the feed mixture. For instance, NaAlg/Co(III)-5 membrane has higher diffusion selectivity, indicating that it is highly selective to water compared to other membranes. This is also in conformity with sorption and flux data of the membranes.

Conclusions

Novel cobalt (III) complex viz., [Co(APABZ)$_2$] Cl·6H$_2$O, was prepared and characterized by X-ray diffraction experiments. The Co(III) complex exhibited water channels in its crystalline lattice and when

Table 4 Diffusion coefficients of water and acetic acid at 303 K for different feed mixtures

Wt.% of water in feed	$D_w \times 10^9$ (m^2/s)	$D_o \times 10^9$ (m^2/s)
Pristine NaAlg		
10	6.7	4.8
20	18.3	15.5
30	24.6	24
NaAlg/Co(III)-2		
10	18.9	5.3
20	32.4	13.2
30	59.6	27.2
NaAlg/Co(III)-3		
10	33.5	8.8
20	49.7	19.8
30	71.6	30.8
NaAlg/Co(III)-5		
10	59.4	10.9
20	74.6	28.6
30	90.6	35.9

Table 5 Pervaporation, sorption and diffusion selectivity data of different membranes at 303 K

Wt.% of water in feed	Pervaporation selectivity (α)	Sorption selectivity (α_S)	Diffusion selectivity[a] (α_D)
Pristine NaAlg			
10	18	13.2	1.4
20	7	6.3	1.1
30	3	3	1
NaAlg/Co(III)-2			
10	64	18.0	3.5
20	24	9.7	2.4
30	13	5.8	2.2
NaAlg/Co(III)-3			
10	79	20.9	3.8
20	28	11.3	2.5
30	15	6.3	2.3
NaAlg/Co(III)-5			
10	174	32.0	5.4
20	40	15.2	2.6
30	19	7.4	2.5

[a] D_α was calculated as: (D_w/D_o)

it was incorporated into NaAlg matrix as a filler in different loadings, the resulting composite membranes offered improved PV performance while dehydrating acetic acid. Among the derived composite membranes, NaAlg/Co(III)-5 composite membrane exhibited a much improved PV performance over that of the pristine crosslinked NaAlg membrane in preferentially extracting water from acetic acid with a selectivity of 174 and a flux of 0.123 kg/m^2 h. These values are higher than those found for pristine NaAlg as well as other composite NaAlg membranes with lower loadings of Co(III) complex particles. The water channels present in Co(III) complex are responsible for this type of effect. Membrane performances have been explained in terms of sorption and diffusion data.

Acknowledgements The authors (T.M Aminabhavi, K.B. Gudasi and R.S. Veerapur) thank University Grants Commission (UGC), New Delhi, India (F1-41/2001/CPP-II) for a major financial support to establish Center of Excellence in Polymer Science (CEPS). This work represents a collaborative effort between CEPS, Dharwad and IICT, Hyderabad under the MoU.

References

1. Gmehling J, Onken U, Arlt W (1981) Vapor–liquid equilibrium data collection, Dechema, Frankfurt/Main
2. Shanley A (September 1994) Chem Eng 101(9):34
3. Aminabhavi TM, Toti US, (2003) Design Monomers Polym 6:211
4. Kurkuri MD, Toti US, Aminabhavi TM (2002) J Appl Polym Sci 86:3642
5. Aminabhavi TM, Naidu BVK, Sridhar S (2004) J Appl Polym Sci 94:1827
6. Naidu BVK, Krishna Rao KSV, Aminabhavi TM (2005) J Membr Sci 260:131
7. Kurkuri MD, Kumbar SG, Aminabhavi TM (2002) J Appl Polym Sci 86:272
8. Uragami T, Saito M (1989) Sep Sci Technol 24:541
9. Mochizuki A, Amiya S, Sato Y, Ogawara H, Yamashita S (1990) J Appl Polym Sci 40:385
10. Yeom CK, Lee KH (1998) J Appl Polym Sci 67:209
11. Huang RYM, Pal R, Moon GY (1999) J Membr Sci 156:101
12. Toti US, Kariduraganavar MY, Soppimath KS, Aminabhavi TM (2002) J Appl Polym Sci 83:259
13. Toti US, Aminabhavi TM (2002) J Appl Polym Sci 85:2014
14. Moon GY, Pal R, Huang RYM (1999) J Membr Sci 156:17
15. Huang RYM, Pal R, Moon GY (2000) J Membr Sci 166:275
16. Wang XN (2000) J Membr Sci 170:71
17. Toti US, Aminabhavi TM (2004) J Membr Sci 228:199–208
18. Kurkuri MD, Toti US, Aminabhavi TM (2002) J Appl Polym Sci 86:3642
19. Yang G, Zhang L, Peng T, Zhong W (2000) J Membr Sci 175:53
20. Lu SY, Chiu CP, Huang HY (2000) J Membr Sci 176:159
21. Lee JF, Wang Y (1998) War Sci Tech 38:463
22. Naidu BVK, Bhat SD, Sairam M, Wali AC, Sawant DP, Halligudi SB, Mallikarjuna NN, Aminabhavi TM (2005) J Appl Polym Sci 96:968
23. Bhat SD, Naidu BVK, Shanbhag GV, Halligudi SB, Sairam M, Aminabhavi TM (2006) Sep Pur Tech 49:56
24. Rat M, Desousa RA, Thomas A, Frapart Y, Tuchagues J, Artaud I (2003) Eur J Inorg Chem 64:759
25. Keene TD, Hursthouse MB, Price DH (2004) Acta Cryst, Sect E60:m381
26. Custelcean R, Afloroaei C, Vlassa M, Polverejan M (2000) Angew Chem 17:39
27. Coleman AW, De Silva E, Nouar F, Nierlich M, Navaza A (2003) Chem Comm:826
28. Ludwig R (2001) Angew Chem Int Ed. 4:1808
29. Crank J (1975) The mathematics of diffusion, Clarenden Press, Oxford
30. Anjali Devi D, Smitha B, Sridhar S, Aminabhavi TM (2005) J Membr Sci 262:91
31. Anjali Devi D, Smitha B, Sridhar S, Aminabhavi TM (2006) J Membr Sci 280:138
32. Fujita H, Kishimoto A, Matsumoto KM (1960) Trans Faraday Soc 56:424
33. Ping ZH, Nguyen QT, Clement R, Neel J (1990) J Membr Sci 48:297
34. Adoor SG, Manjeshwar LS, Naidu BVK, Sairam M, Aminabhavi TM (2006) J Membr Sci 280:594
35. Naidu BVK, Shetty LC, Aminabhavi TM (2004) J Appl Polym Sci 92:2740